First High Fluence Irradiation Tests of Lasers for Upgraded CMS at SLHC

M.Axer, S.Dris, K.Gill, R.Grabit, E.Noah, R.Macias-Jareno, J.Troska, F.Vasey

PH-MIC-OE, CERN, 1211 Geneva 23, Switzerland
Markus.Axer@cern.ch

Abstract

An irradiation test of five lasers of the type used in the current CMS Tracker optical links was made with a neutron fluence of $4x10^{15}n/cm^2$, simulating the conditions of an upgraded CMS Tracker operating at SLHC. The usual radiation effects were observed, though with the ultimate failure point of the devices being seen for the first time. The laser lifetime was limited by thermal performance as much as radiation damage. With appropriate cooling these lasers could be suitable for optical link applications in an upgraded CMS Tracker. In addition a streamlined irradiation test procedure can be envisaged in future for high fluence testing.

I. INTRODUCTION

Analogue and digital optical link systems have been developed at CERN[1] to read out and control more than 16.000 silicon strip detector modules in the CMS Tracker. Over the first ten years of LHC operation, the silicon detectors, electronics, optical links, and other materials used in the Tracker will be exposed to fluences of up to $2x10^{14}particles/cm^2$ (dominated by pions with ~200MeV) and ionizing doses of up to 100kGy.[2] The optical link parts inside CMS are also expected to be inaccessible over a period of up to 10 years. Both radiation hardness and reliability are therefore important issues of concern and an extensive series of qualification and advanced validation tests[1] were made to confirm the suitability of commercial off-the shelf (COTS) optical link components for the CMS optical links. In this context the functionality of lasers was validated for fluences equivalent to $2x10^{14}pions/cm^2$ (200MeV pions) and ionizing doses of 100kGy. It was shown also that the damage due to 200MeV pions is about twice as high as the damage caused by neutrons of ~20MeV in the irradiation facility used in the present tests.[3]

In view of the proposed upgrade of the LHC machine towards Super-LHC (SLHC), as well as upgrades of the CMS detector, the effect of a 10-fold increase in luminosity to $10^{35}cm^{-2}s^{-1}$ is considered in this paper. The radiation environment is expected to be about ten times more intense than that considered in the current generation of the optical links. Testing is therefore required at dose levels of 1 MGy and fluences in excess of $2x10^{15}particles/cm^2$, where the dominant particle species is expected to remain charged pions with energies around 200MeV. Work has started at CERN to investigate optical link components for this more demanding application. A first irradiation test has been made at the end of the year 2004 using a neutron source to very high fluences in order to assess the potential to re-use already existing optical link components in an upgraded CMS Tracker at SLHC. The experience and results gained during the testing were also analyzed with a view to evolving the current test procedure towards future component validation and qualification for SLHC applications.

II. HIGH FLUENCE NEUTRON IRRADIATION

A. Devices Under Test

Five laser transmitters of the same type as those used in the current CMS optical link generation were irradiated. These devices are 1310 nm InGaAsP/InP multi-quantum-well edge-emitters produced by Mitsubishi (type ML7CP8), die packaged and provided by ST Microelectronics in a compact fibre-pigtailed assembly.[1]

B. Test Method

The T2 neutron irradiation facility of the Cyclotron Research Center (CRC) at the Université Catholique de Louvain (UCL) was used for the irradiation.[4] An intense neutron beam is available with an average energy of about 20MeV, originating from a beryllium target bombarded with 50MeV deuterons. Dosimetry was made by comparing the integrated beam current with previous calibration measurments. The accuracy of the dosimetry was 20%.[4] The target neutron fluence was $4x10^{15}n/cm^2$ which was reached after 22hrs of exposure.

The lasers under test were connected both optically and electrically in order to measure the radiation damage and annealing effects in situ. The actual laser temperature (the junction temperature T_j) was also measured, for the very first time in one of the irradiation tests. The surrounding ambient air temperature T_{amb} was maintained constant using a controllable ventilation system.

Figure 1 shows the measurement system. It was separated into two parts, the first (uppermost in Figure 1) was based upon a system used in previous irradiation tests[3] and this was used to monitor the light output power-current (L-I) and voltage-current (V-I) characteristics of three lasers LD1 to LD3 at periodic intervals, during and after irradiation. The second part of the setup (lowermost in Figure 1) was based on that used already for the studies of temperature effects on the wavelength spectrum and measurements of the thermal resistance of lasers in the laboratory. Two lasers, LD4 and LD5, were used to monitor the temperature effects throughout the test exclusively.

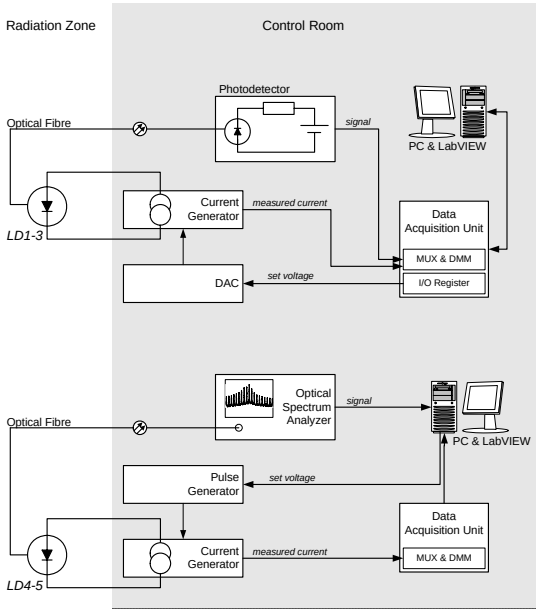

Figure 1: Control and data acquisition systems for in-situ measurements of L-I characteristics (top) and wavelength spectra (bottom).

Figure 2 illustrates the most important parameters extracted from an L-I characteristic: the threshold current I_{th}, which is the drive current at which a laser starts to emit coherent light, and the output efficiency Eff, which is the slope of the linear part of the L-I above threshold. The laser threshold current and efficiency are affected by radiation damage, in particular displacement damage rather than ionization damage.[3] Some fraction of the radiation damage usually recovers (anneals) already during irradiation and the annealing continues after irradiation with a rate that is dependent upon both the temperature and bias current.[3]

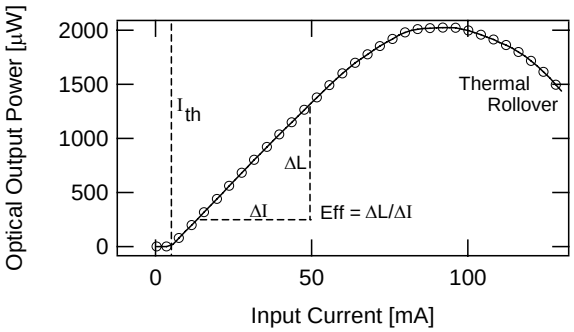

Figure 2: Typical L-I characteristic of an un-irradiated laser operated at room temperature.

At high input currents the L-I characteristic becomes nonlinear and exhibits 'thermal rollover'. Operating a laser diode at high currents causes the device to heat up significantly, resulting in a decrease of the light output power since non-radiative recombination mechanisms become more and more dominant. For InGaAsP/InP lasers Auger recombination, which increases with greater carrier concentration and higher temperature, is expected to be the dominant mechanism causing the rollover.[5]

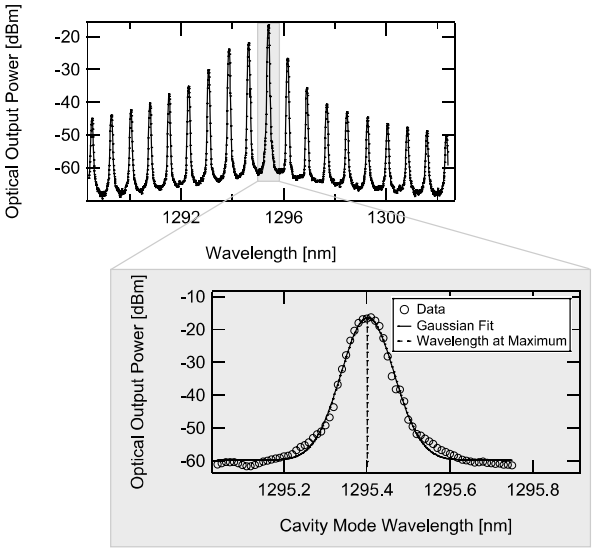

Figure 3: Section of a Fabry-Perot laser wavelength spectrum as measured with an Optical Spectrum Analyzer (top). Each cavity mode can be measured very precisely with a resolution of 10pm (bottom).

The energy band-gap, the refractive index as well as the cavity length of a laser die are sensitive to the temperature. Since these properties affect the emitted wavelength spectrum then a change in the internal device (junction) temperature T_j can be determined from observation of the emitted wavelength spectrum (Figure 3). The difference between the junction temperature and the ambient value is determined by the thermal resistance of the device, which relates the internal temperature to the power dissipation according to:

$$R_{th} = \frac{\Delta T}{P_{diss}} = \frac{T_j - T_{amb}}{P_{in} - P_{opt}} \approx \frac{T_j - T_{amb}}{P_{in}}, \qquad \textit{Equation } 1$$

where ΔT is the temperature difference between the junction and the ambient temperature T_{amb}. P_{diss} is the thermally dissipated power within the laser defined by the electrical input power P_{in} minus the optical power P_{opt}. R_{th} therefore describes the device's resistance to release heat generated at the laser diode junction. Most of the emitted optical power P_{opt} is in fact absorbed by the laser package (only a small fraction is coupled into the fibre), therefore we assume $P_{diss} = P_{in}$ as in Equation 1. If R_{th} is known for a given laser then the junction temperature under specific operating conditions can be determined (or vice versa). The value of the thermal resistance is heavily affected by the thermal conductivity of the materials used and the mounted configuration. In other words, the thermal resistance characterizes in fact the entire device assembly working in a given environment.

We therefore determined R_{th} from in-situ wavelength measurements made during the irradiation. The effects of ambient temperature and input power on the spectrum in terms of the slopes $\Delta\lambda/\Delta P_{in}$ and $\Delta\lambda/\Delta T_{amb}$ are correlated through the thermal resistance:

$$R_{th} = \frac{\Delta\lambda / \Delta P_{in}}{\Delta\lambda / \Delta T_{amb}}, \qquad \textit{Equation } 2$$

where this equation holds for the shifting gain envelope and the shift of each individual cavity mode. As shown in Figure 3, individual cavity modes could be very precisely measured (and fitted with a gaussian). With some care, we were able to track the wavelength changes associated with a particular mode (measuring the position of the peak of the fitted gaussian curve) throughout the entire irradiation test.

The effect of ambient temperature on the wavelength is in fact the same for all lasers with the same material system and so $\Delta\lambda/\Delta T_{amb}$ is a constant. This value was measured in the laboratory before and after irradiation (on devices that were irradiated in an earlier test to fluences of $4x10^{14}n/cm^2$). A controllable oven was used to vary the ambient temperature whilst the change of the wavelength spectrum was monitored. Measurement of several laser diodes confirmed that $\Delta\lambda/\Delta T_{amb}$ was indeed constant with an average value of 0.09nm/°C. An additional interesting result was that the thermal resistance was also unaffected by radiation damage.

In this high fluence test it was therefore sufficient to monitor only the effect of changing input power on the wavelength spectrum $\Delta\lambda/\Delta P_{in}$ in order to derive T_j according to:

$$T_j = \frac{P_{in} \cdot (\Delta\lambda / \Delta P_{in})}{0.09nm/°C} + T_{amb} \quad . \qquad Equation\ 3$$

III. RESULTS

The initial laser threshold currents were around 5mA at 20°C whilst the output efficiencies were ~40μW/mA for LD1 and ~15μW/mA for LD2 and LD3, as specified according to their application in CMS in the analogue or the digital optical link system respectively. The initial wavelengths of LD4 and LD5 were chosen to be the maxima positions of the lasing peaks, those cavity modes with the highest light output (λ_{LD4}=1309.56nm and λ_{LD5}=1312.59nm at ~20°C).

A. Radiation Damage

Figure 4 illustrates how the L-I characteristics typically changed during the neutron irradiation. With increasing fluence both the threshold current increase and the efficiency loss are evident. Likewise the thermal rollover starts to become visible in the measurements at high fluences where the input currents are becoming large. In excess of about $3x10^{15}n/cm^2$ the laser fails and the device behaves like an LED. This is shown more clearly in Figure 5 where the power output (with all the L-I data during irradiation) for LD1 are displayed on a log scale. The device failures however were essentially related to the high fluence test procedure and this failure is only temporary and is reversed by the annealing that takes place after irradiation (see section IV). The symmetry of the thermal rollover is also remarkable and this feature hints at a new streamlined test method (described in section V).

The extracted values for the threshold current I_{th} and the relative change of efficiency Eff_{rel} (actual efficiency normalized to the initial efficiency) for all three laser diodes tested are displayed in Figure 7 as a function of neutron fluence. The evolution of radiation damage was almost linear with neutron fluences up to $3x10^{15}n/cm^2$ after which the L-I curve was difficult to fit reliably.

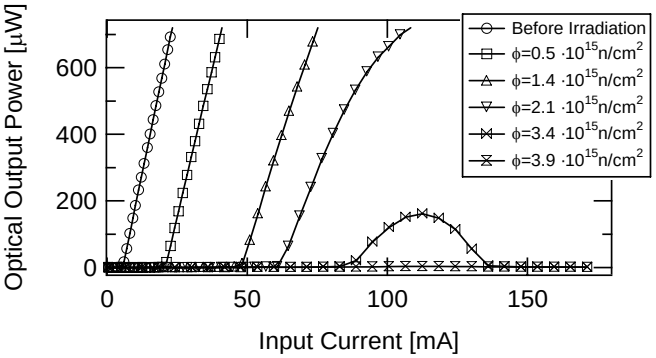

Figure 4: Subset of typical L-I characteristics observed at different neutron fluences. The examples are results from laser LD1.

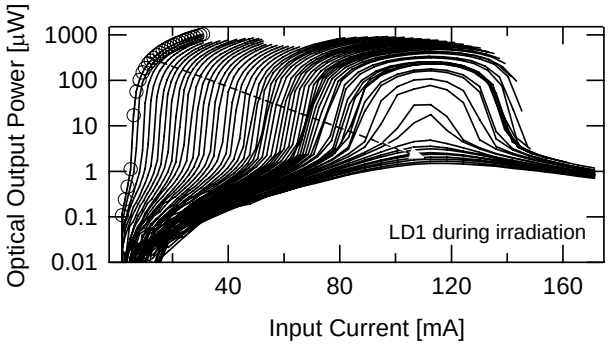

Figure 5: All L-I characteristics measured for LD1 during irradiation with power output on a log scale. The arrow indicates the direction of time. For comparison the L-I result obtained before irradiation is also included (circular markers).

After an exposure time of about 3hrs a fluence of $5x10^{14}n/cm^2$ was reached and the results could be compared to those obtained in earlier tests to this fluence that were performed under similar conditions of bias and temperature[3]. As in the earlier tests the thresholds increased by about 20mA and the efficiency losses were around 20%.

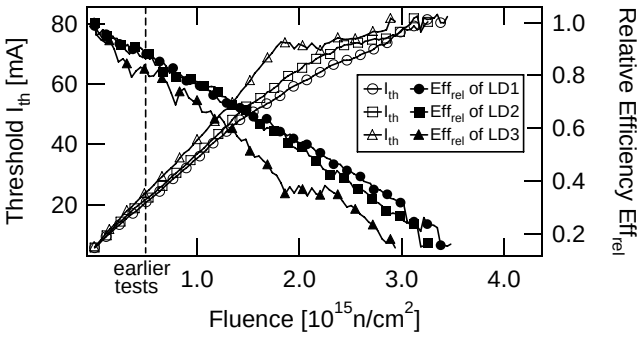

Figure 6: Measured threshold current I_{th} and relative efficiency Eff_{rel} versus neutron fluence for LD1-3. A reasonable extraction of both parameters above ~$3x10^{15}n/cm^2$ was not possible.

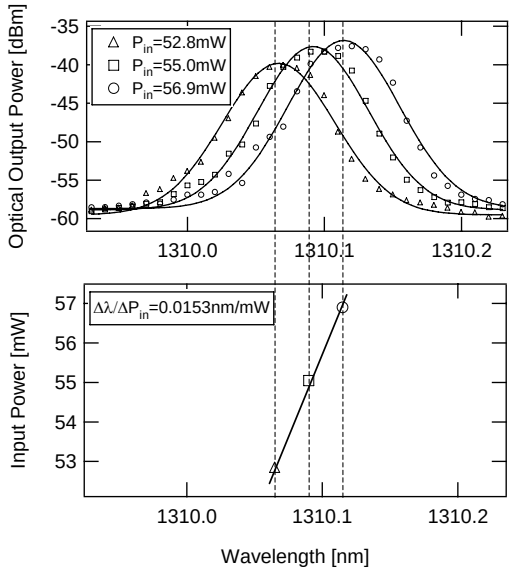

Figure 7: Typical cavity mode wavelength shift due to the increase of input current (input power) as observed during irradiation.

B. Thermal Effects

The effect of changing input power on a specific cavity mode wavelength is shown in Figure 7. In this illustrative example only three measurements from LD4 are displayed. Taking all measurements into account, the value of $\Delta\lambda/\Delta P_{in}$ was 0.0153nm/mW and R_{th} was 170°C/W. The result for LD5 was similar and therefore the above value of thermal resistance was used for all five laser diodes. It is noted however that $\Delta\lambda/\Delta P_{in}$ might vary from laser to laser due to slightly different thermal conditions, e.g. the thermal conductivity of the particular laser-hybrid assembly.

The internal laser junction temperature at threshold was determined using Equation 3. Figure 8 shows the evolution of T_j for LD1 determined for the input power at threshold current in comparison to the measured ambient temperature T_{amb}. This result is representative for all lasers tested as they were operated under the same conditions. Because of the thermal resistance the lasers were in fact operating at about 42°C (when driven at the threshold current) at the end of irradiation despite being at an ambient temperature of 20°C.

It is interesting to consider the effect of this self-heating on the radiation damage results. For example the threshold current I_{th} is known to vary (approximately) with temperature according to

$$I_{th}(T_1) = I_{th}(T_2)\exp\left(\frac{T_1 - T_2}{T_0}\right), \qquad \textit{Equation } 4$$

with T_0=65K being the characteristic temperature.[5] This formula was used to normalize the measured threshold damage results to a temperature T_1=20°C. Figure 9 (top) shows the evolution of I_{th}(20°C) for cases in which $T_2=T_{amb}$ (i.e. ignoring the self-heating) and $T_2=T_j$ respectively. The effect of internal heating on the radiation damage is clear. Figure 9 (bottom) illustrates the percentage thermal contribution to the change of threshold current expressed by $\text{Therm}(I_{th})=I_{th}(T_2=T_{amb})/I_{th}(T_2=T_j)$-1. The results are similar for all three lasers tested. Towards the end of the irradiation about 40% of the measured threshold shift was due to the internal device temperature. It is also noted that, after a fluence of $1.5\text{x}10^{15}$n/cm^2, the rate of threshold increase slows down (when considering the data that has been corrected for self-heating) and this is most likely due to the competition with beneficial annealing processes that are taking place during the irradiation.

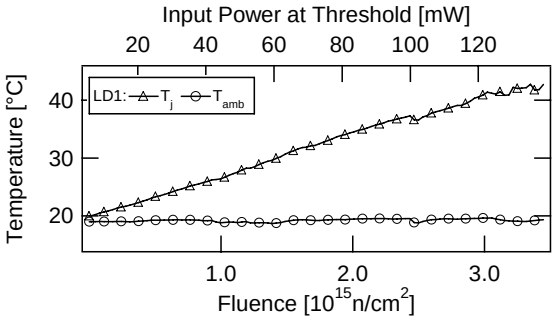

Figure 8: Extracted junction temperature T_j and measured ambient temperature T_{amb} for LD1 as a function of input power at threshold and fluence, respectively.

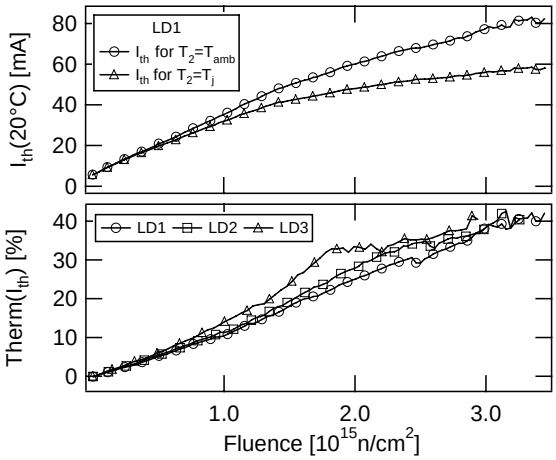

Figure 9: Threshold data for LD1 normalized to T_1=20°C according to Equation 3 as a function of fluence (top). Thermal contributions to the change of threshold current observed for LD1-3 (bottom).

IV. THE ULTIMATE LIFETIME OF THE LASERS

The ultimate lifetime of the lasers in this test appears to be affected as much by the internal junction temperature of the laser, as by the radiation damage. The effects are synergistic: after being damaged, more current is required to drive the laser and this, in turn, heats the device and the light output at higher currents then also decreases. It is clear from the results shown in Figure 5 that under these test conditions the threshold current increase was limited to a maximum value of around 100mA, at which point the laser fails.

The important question is therefore whether the radiation damage under SLHC conditions would cause a 100mA

threshold shift (or 100% efficiency loss). To address this question it is necessary to consider the effects of annealing (and temperature) more closely, since this has a significant impact on the net damage, particularly over longer irradiation periods.

In this particular test, measurements were continued for 200 hours after irradiation in order to monitor any annealing. Figure 10 shows the results for LD1. The degree of annealing is significant and the device soon recovers to operate again as a laser. These measurements are very encouraging and they indicate that there is a flux dependence of the damage and that much less damage would result if the same fluence was accumulated over a longer irradiation period. Previous studies[3] on the same lasers suggested that the radiation damage to lasers in the CMS Tracker over the first 10 years of running under 'standard' LHC conditions would be 70% less than that observed in a test to the same equivalent fluence in the T2 facility, due to the annealing that would occur during this time.

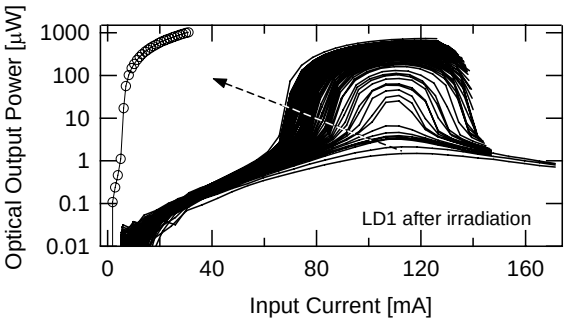

Figure 10: L-I characteristics measured for LD1 after irradiation in log scale presentation. The arrow indicates the direction of time. For comparison the L-I result obtained before irradiation is also included (circular markers).

The important effect of self-heating seen in Figure 9 also suggests that R&D into improved sub-mounts for the lasers, to maximize heat transfer away from the laser and reduce R_{th}, would be very worthwhile and may increase the lifetime of the devices in terms of radiation hardness. In this way we might be able to recover some of the 40% of the observed damage that was due to internal heating. However, the synergistic effects governing the radiation damage will have to be considered carefully, since if the junction temperature is reduced the annealing will also be slowed down. A model of the damage, annealing and heating effects would, in addition, be very useful in order to determine the ideal R_{th} and the levels of damage that could be expected for lasers at different positions in an upgraded Tracker at SLHC.

V. STREAMLINING OF FUTURE TESTS

The combined radiation damage and thermal results suggest that a streamlined method could be used for future SLHC-oriented radiation hardness validation tests. The radiation damage at high fluences could be inferred from low fluence data by making a study of the thermal rollover all the way through the irradiation test (as in Figure 11). The ultimate maximum threshold current $I_{th,max}$ that could be reached under high fluence conditions before the laser fails should then be visible even after a short irradiation to a relatively low fluence. Such streamlining would minimize the time, costs and complexity of SLHC radiation testing of lasers, and it would relax the choice of irradiation facilities, and reduce problems of handling radioactive samples.

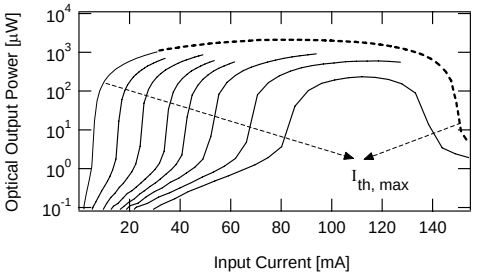

Figure 11: Low fluence irradiation tests in combination with a complete thermal characterization can be used to predict the laser behaviour under very high fluences.

VI. CONCLUSIONS

Five lasers of the type used in the current CMS Tracker optical links were irradiated to neutron fluences of $4x10^{15}n/cm^2$ simulating conditions in an upgraded Tracker at SLHC. A specific technique to monitor the device internal temperature based on wavelength spectrum measurements was used besides the usual radiation damage measurements. In addition to the typical threshold increase and efficiency loss, the ultimate failure point of the devices was measured for the first time. The laser lifetime was limited as much by thermal performance as by radiation damage in this test. In a much longer irradiation, such as the real CMS Tracker application, the damage would be expected to be much smaller such that the lasers probably would not fail due to radiation damage. A streamlined test procedure can be envisaged in future, as well as ways to improve the device radiation resistance by dedicated cooling.

VII. ACKNOWLEDGEMENTS

We would like to thank the staff of CRC, in particular Eric Forton, for their assistance with the irradiation. Christophe Sigaud of CERN is thanked for his help in preparing the test instrumentation.

VIII. REFERENCES

[1] CMS Optical links projects at CERN, information available online: http://cms-tk-opto.web.cern.ch.
[2] M. Huhtinen, "Radiation Environment in (CMS) Experimental Area", RD49 Course on radiation effects, 2000, http://rd49.web.cern.ch/RD49/MaterialRadCourse/MHuhtinen2.pdf.
[3] K. Gill et al., "Combined radiation damage, annealing and ageing studies of InGaAsP/InP 1310nm lasers for the CMS Tracker optical links", Ref. Conference on Photonics for Space Environments VIII, SPIE Vol. 4823, pp. 19-33, 2002.
[4] T2 neutron beam facility at UCL, Louvain-la-Neuve, Belgium, information available online: http://www.fynu.ucl.ac.be/themes/he/cms/neutron_beam/neutrons.html.
[5] G.P. Agrawal, N.K. Dutta, "Semiconductor Lasers", 2nd Edition, Van Nostarnd Reinhold, ISBN 0-442-01102-4, 1993.